Supporting Information for

Heterometallic Metal-organic Framework Nanocages of High Crystallinity: Elongated Channel Structure Formed *in-situ* Through Metal-ions (M=W or Mo) Doping

Jinxin Wei,[ab] *Niancai Cheng,*[ab] *Zhiyu Liang,*[ab] *Yufeng Wu,*[ab] *Zhigang Zou,*[bc] *Zanyong Zhuang,**[ab] *and Yan Yu**[ab]

[a]College of Materials Science and Engineering, Fuzhou University, New Campus, Minhou, Fujian 350108, China

[b]Key Laboratory of Eco-materials Advanced Technology (Fuzhou University), Fujian Province University, Fuzhou, Fujian 350108, China

[c]Jiangsu Key Laboratory for Nano Technology, Nanjing University, Nanjing 210093, China

* E-mail: zyzhuang@fzu.edu.cn, yuyan_1972@126.com

Supplemental Figures and Discussions

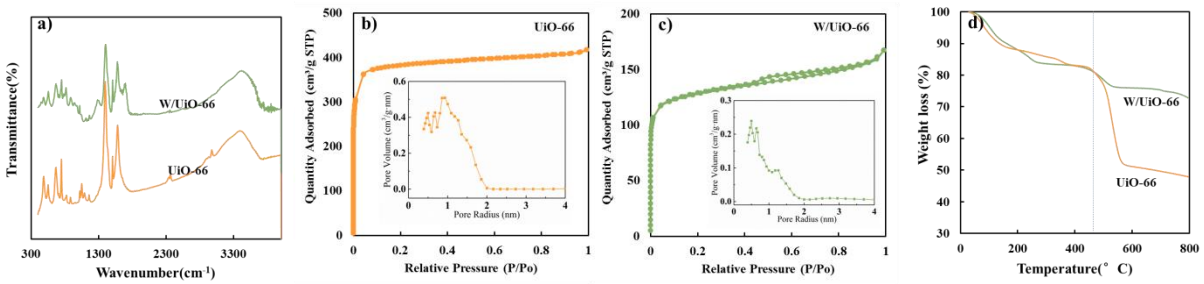

Figure S1. (a) FT-IR spectra, (b,c) N_2 adsorption-desorption isotherms curves and the corresponding pore size distribution curves, and (d) TGA curves of UiO-66 and W/UiO-66.

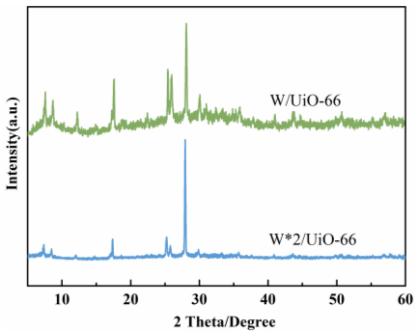

Figure S2. XRD patterns of W/UiO-66 and W*2/UiO-66 nanocages.

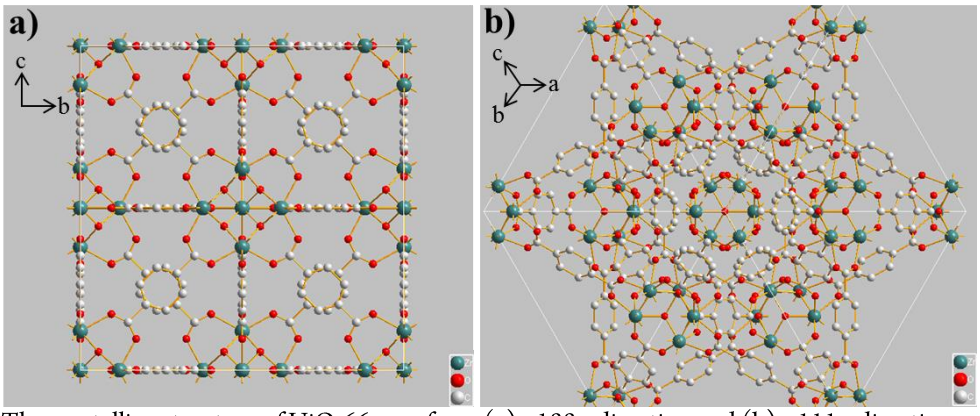

Figure S3. The crystalline structure of UiO-66 seen from (a) <100> direction and (b) <111> direction, respectively.

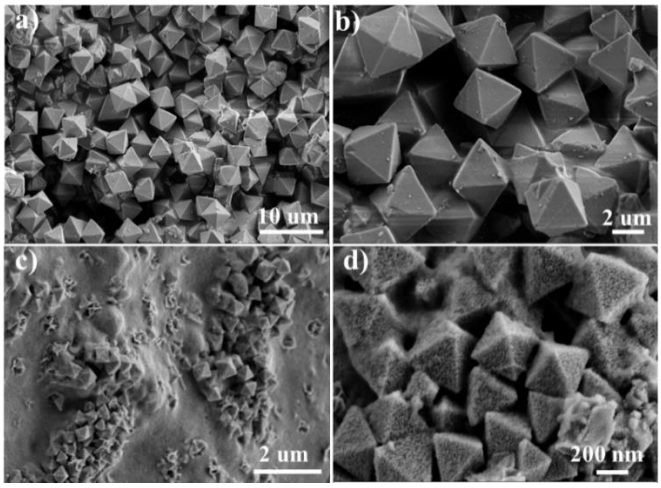

Figure S4. SEM images of solid UiO-66 (a,b) immersed in acid solution or (c,d) immersed in Na_2WO_4 solution at 180 °C for 4 h.

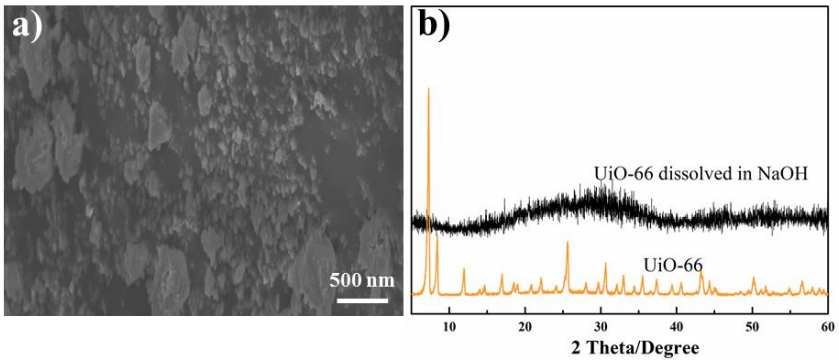

Figure S5. (a) SEM picture of the UiO-66 dissolve in alkaline solution; XRD patterns of UiO-66 dissolved in NaOH compared with UiO-66.

Investigation of the phase of W in cages

Unfortunately, we found that despite the abundance of W in nanocages, there was not any lattice fringe of WO_3 observed in the HRTEM images of the nanocages. To detect the WO_3, Raman spectra and diffuse reflectance spectra (DRS) were recorded. Figure S4a,b shows that compared with fresh UiO-66, the W/UiO-66 nanocages contained a new Raman peak at 960–970 nm^{-1}, which differed from the peak of Na_2WO_4 (931.5 nm^{-1}) and could be attributed to 2 nm WO_3 (964 nm^{-1}).[1] The occurrence of WO_3 was further supported by UV-vis analysis. Figure S5 shows that the absorption edge of the nanocages was between that of pure WO_3 (450 nm) and UiO-66 (340 nm), which indicated a hybrid of WO_3 and UiO-66. Furthermore, after the formation of nanocages, there were fewer micropores whose size was less than 2 nm (Figure S6), which also well agreed with the filling of newly-formed WO_3 particles in micropores of UiO-66. All these results could support our hypothesis that WO_4^{2-} reacted with UiO-66 during the formation of nanocages.

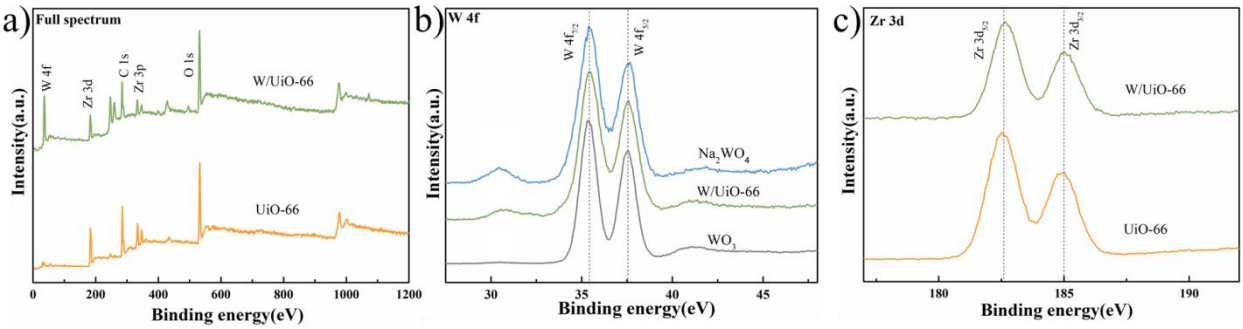

Figure S6. (a) Survey XPS spectra and (b) high-resolution XPS spectra of W 4f peaks of Na_2WO_4, W/UiO-66, and WO_3. (c) The high-resolution XPS spectra of Zr 3d peaks of UiO-66 and W/UiO-66 nanocages.

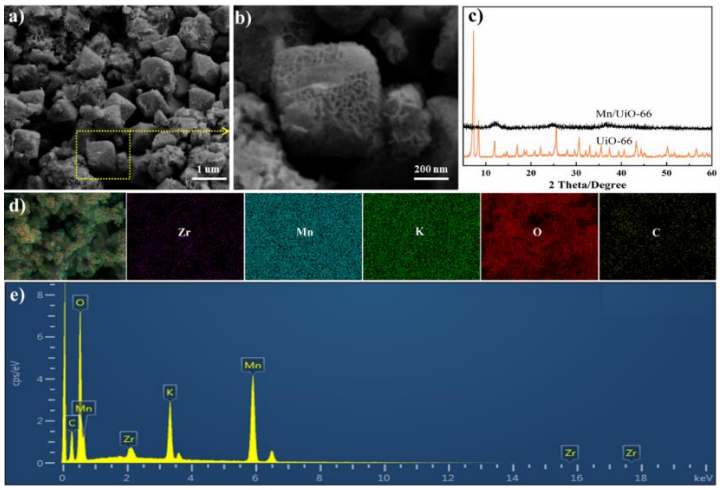

Figure S7. (a, b) SEM images of Mn/UiO-66; (c) XRD patterns of pristine UiO-66 and Mn/UiO-66; (d) elemental mapping images of Zr, Mn, K, O, C in the Mn/UiO-66; (e) EDS pattern of Mn/UiO-66.

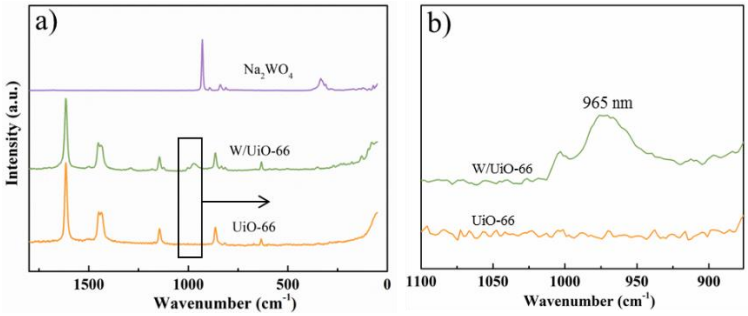

Figure S8. (a) Raman spectra of Na_2WO_4, W/UiO-66, and UiO-66; (b) Raman spectra of samples with wavenumber ranging from 900 to 1100 cm^{-1}.

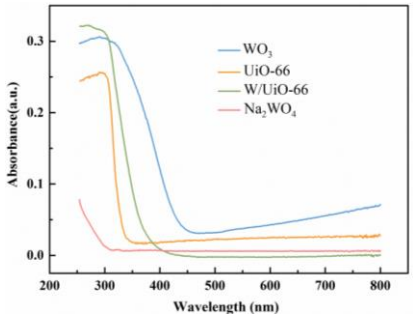

Figure S9. Diffuse Reflectance Spectra (DRS) of UiO-66, W/UiO-66, WO_3, and Na_2WO_4.

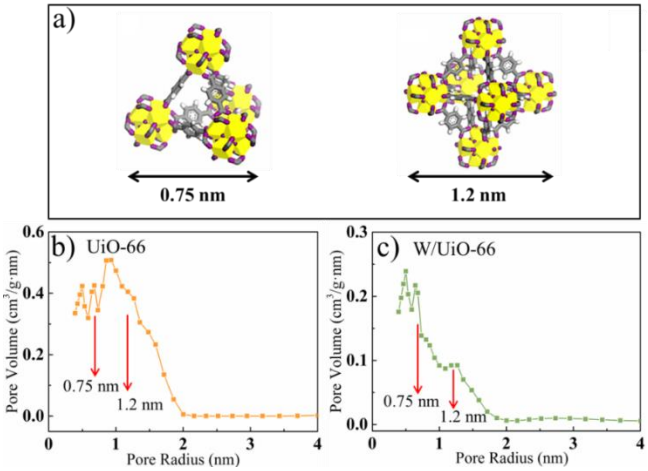

Figure S10. (a) Owing to its intrinsic structural features, UiO-66 contained both tetrahedral and octahedral pores, which had distinctive dimensions of 0.75 and 1.2 nm, respectively. (b, c) shows that although the <0.72 nm micropores were preserved after the incorporation of W into UiO-66, the ~1.2 nm pores were lost significantly. This loss indicated that small particles accumulated inside the octahedral pores.

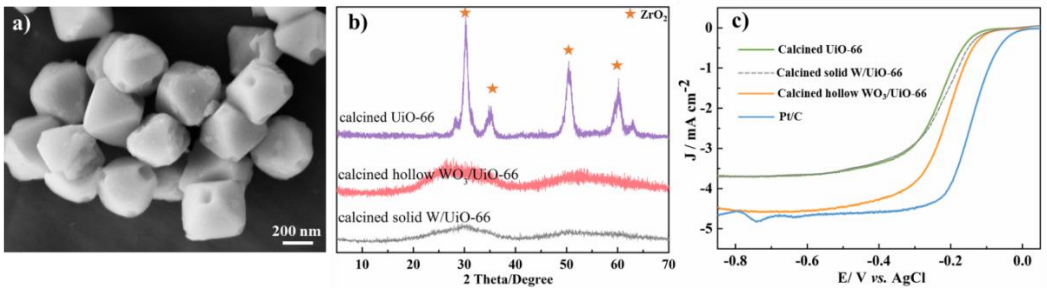

Figure S11. (a) SEM image of calcined WO_3/UiO-66 collected at etching time of 2h; (b)XRD patterns and (c) LSV curves of annealed UiO-66, WO_3/UiO-66, and W/UiO-66 collected at t=2 h. Pt/C was set as a comparison with the above three samples in ORR activity.

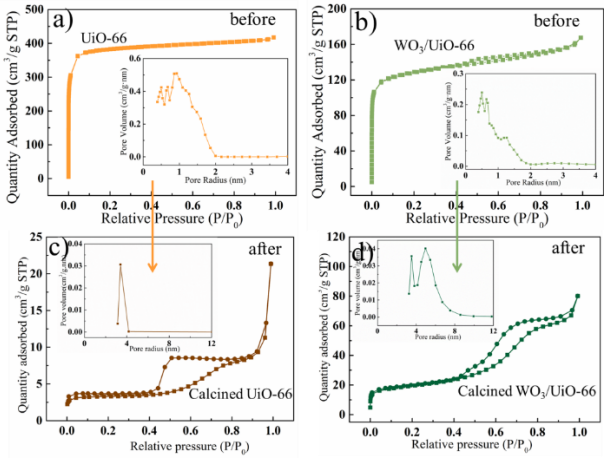

Figure S12. N_2 adsorption-desorption isotherms and the corresponding pore size distribution curves of (a) UiO-66, (b) WO_3/UiO-66, (c) calcined UiO-66, and (d) calcined WO_3/UiO-66.

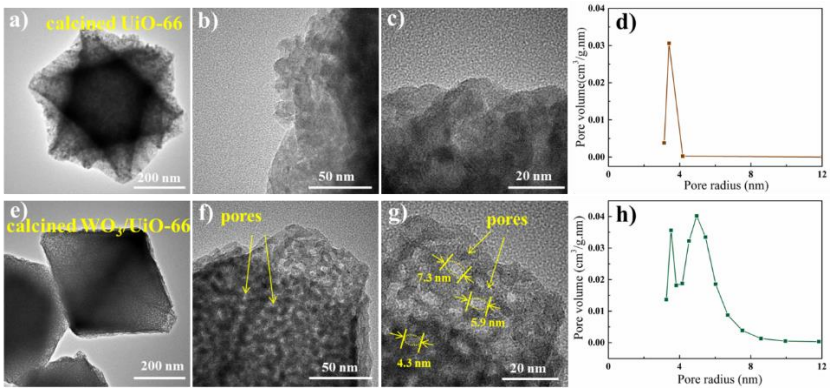

Figure S13. (a–c) TEM images of calcined UiO-66; (d) The corresponding pore size distribution curve of calcined UiO-66; (e–g) TEM images of calcined WO_3/UiO-66; (h) The corresponding pore size distribution curve of calcined WO_3/UiO-66.

References

1. M. Boulova and G. Lucazeau, *J. Solid. State. Chem.*, 2002, **167**, 425-434.